Supplementary Information

Alejandro Martínez-García[a,b], Venkat Kalyan Vendra[a,b], Swathi Sunkara[a,b], Poonum Haldankar[c] , Jacek Jazinski[b], and Mahendra K. Sunkara[a,b]

Phase pure Cu_2O was synthesized by annealing copper hydroxide nanowires in N_2 for 4 hours the copper oxide. Figure S.I shows the structural, optical and photoelectrochemical characterization of electrodes comprising phase pure Cu_2O only.

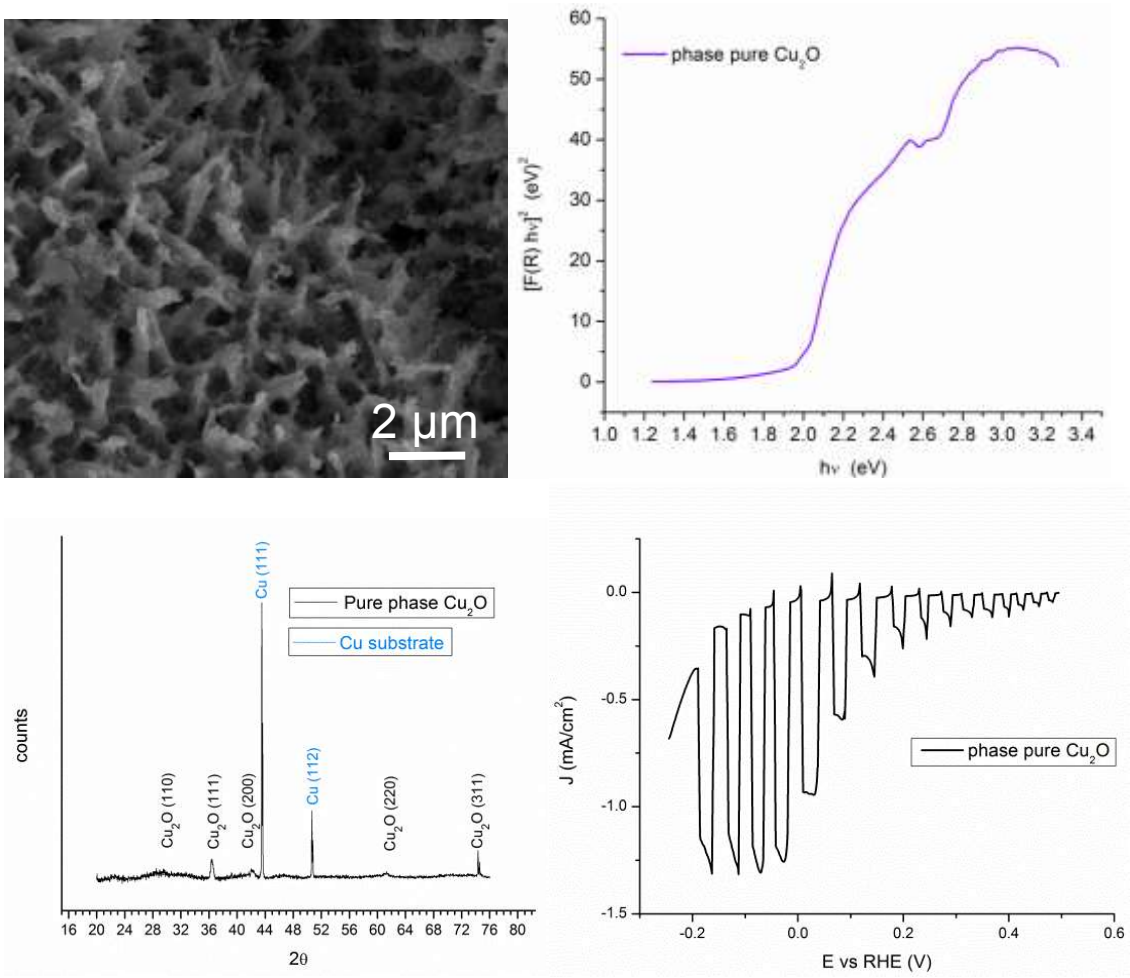

Figure S.I. *Phase pure Cu_2O a) SEM (tilt 45º), b) Tauc Plot, c) XRD, d) Linear Sweep Voltammetry, at pH 5.*

Figure S.II shows a transient open circuit voltage for two Cu_2O samples coated with WO_3 (black) and $CuWO_4$ (red) deposited by hot filament CVD . The open circuit potential under illumination becomes more positive, suggesting the electrode has a p-type conductivity.

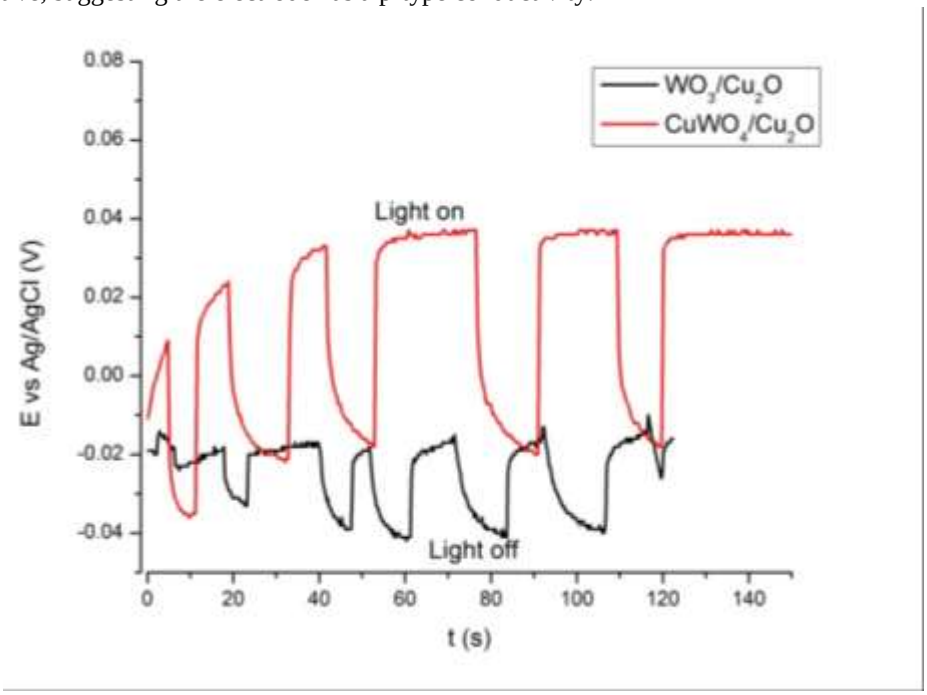

Figure S.II. *Transient open-circuit voltage for the $CuOW_4$, WO_3 coated Cu_2O NWs.*

Figure S.III shows the linear sweep voltammetry of Cu_2O/WO_3 electrodes with different WO_3 deposition times. At voltages near the onset potential, where band bending is low, spikes in photocurrent are observed under illumination. These spikes are less intense in the electrodes having thicker WO_3 coatings. This can be understood by considering the extent of the depletion in Cu_2O for different WO_3 thickness. If the thickness of the WO_3 layer is less than the depletion region width in WO_3, then the space charge region in the p-Cu_2O needs to become smaller in order to maintain the charge neutrality. By contrast, for a WO_3 layer that exceeds the depletion region in the n-type WO_3, the space charge in p-Cu_2O is larger than for the thin WO_3 case. Therefore, the band bending for p-Cu_2O is more intense for thicker tungsten oxide coatings. Consequently, the accumulation of electrons in Cu_2O coated with thick WO_3 is not as prevalent and surface recombination is limited. The foregoing also accounts for improved stability in the thicker samples, since less excess electrons are accumulated in Cu_2O that could reduce the semiconductor to metallic copper.

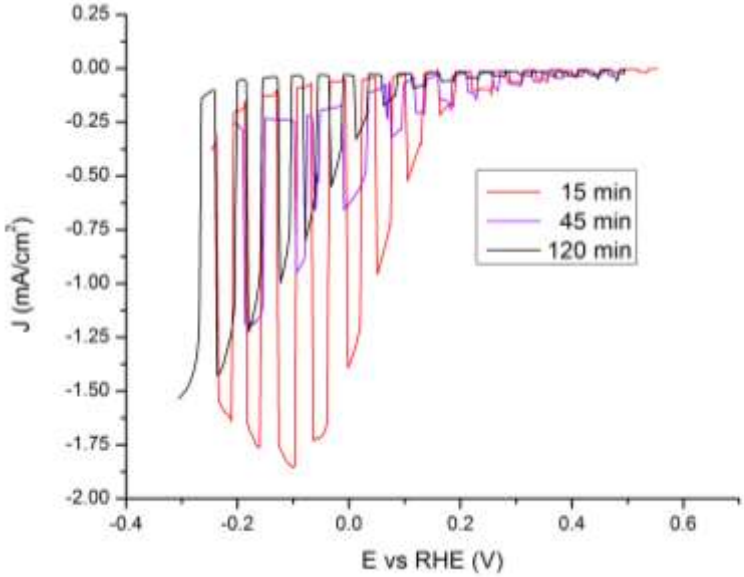

Figure S.III. *Linear Sweep Voltammetry for Cu_2O/WO_3; 15 min deposition of WO_3 (red), 45 min deposition of WO_3 (purple), 120 min deposition of WO_3 (black).*

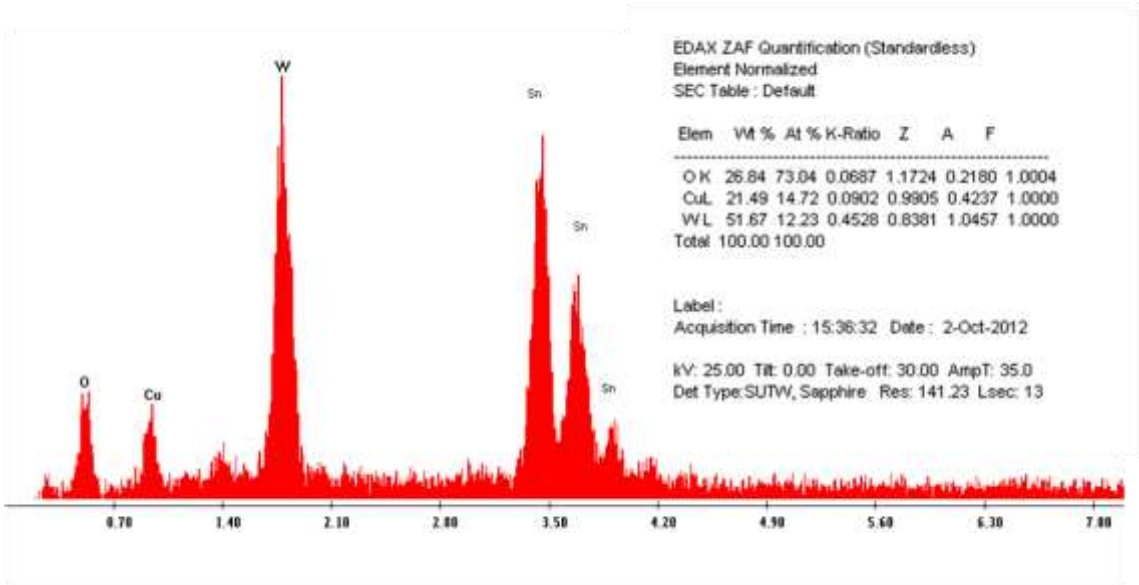

Figure S. IV. *Energy Dispersive X-Ray Spectrum (EDS) of $CuWO_4$ film on FTO. Inset: Elemental composition analysis of film showing a 1:1 atomic ratio of Cu to W. Sn peaks from underlying FTO.*

The EDS data presented in figure S.IV was obtained from a film deposited by HFCVD with the copper-tungsten filament assembly on fluorinated tin oxide coated glass . The elemental quantification shows that the atomic ratio of Copper to Tungsten is around 1:1. This ratio is consistent with the stoichiometry of $CuWO_4$. The Sn signals result from the underlying tin oxide.

Figure S.Va shows a sketch of the HWCVD system used to deposit WO_3 and $CuWO_4$. This image shows how the substrates were positioned underneath the metal source filament for deposition. The quartz tube is maintained at low pressure by a rotary vane vacuum pump and oxygen is fed through a gas distribution system depicted in the upper left hand side. Figure S.Vb shows the filament assembly in detail: a thicker tungsten filament is wrapped with a thinner copper wire as sources of these metals for the deposition of copper tungstate.

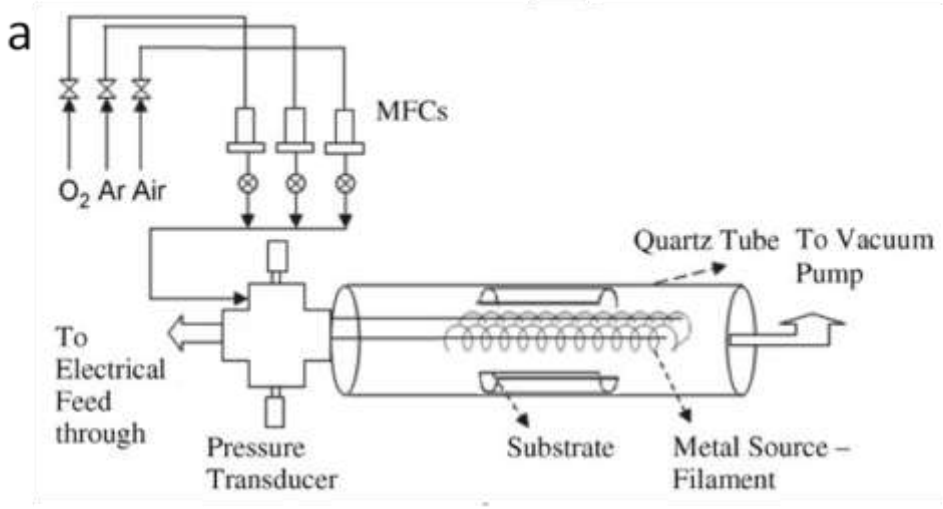

Figure S. V *a) Sketch of HFCVD reactor used for deposition of WO_3 or $CuWO_4$. b) macroscopic photograph of tungsten-copper filament assembly used for deposition of $CuWO_4$.*

Figure S.VI presents a model for the deposition of WO_3 and simultaneous reduction of CuO nanowires to Cu_2O. The volatile reducing agent is shown as it is transported from the hot tungsten filament after reaction with O_2. The nucleation of WO_2 and uptake of oxygen from the wires is believed to be the mechanism by which a WO_3 shell and Cu_2O core form simultaneously.

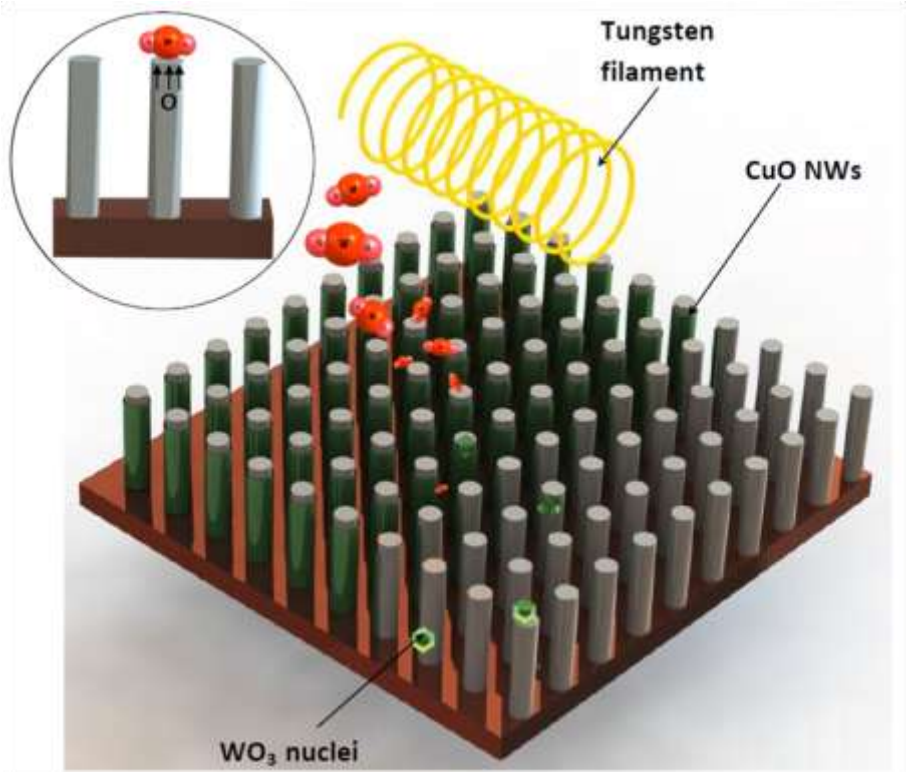

Figure S. VI *a) Redox model for copper oxide phase transformation.*